Title: Simultaneous scalp recorded EEG and local field potentials from monkey ventral premotor cortex during action observation and execution reveals the contribution of mirror and motor neurons to the mu-rhythm

Authors: Marco Bimbi [1], Fabrizia Festante [1], Gino Coudé [1,2], Ross E. Vanderwert [3], Nathan A. Fox [4] and Pier Francesco Ferrari [1,2]

Affiliations: [1] Dip. di Medicina e Chirurgia, Università di Parma, Parma, 43125, ITALY; [2] Institut des Sciences Cognitives Marc Jeannerod, CNRS, Bron, Cedex 69675, France; [3] School of Psychology, Cardiff University, Cardiff, CF10 3AT, UK; [4] Dept. Of Human Development and Quantitative Methodology, University of Maryland, College Park, 20740, USA.

Corresponding author: Pier Francesco Ferrari,

email: pff@isc.cnrs.fr

work phone number: +33 4 37911226

Address: Institut des Sciences Cognitives Marc Jeannerod-CNRS, 67 Bd Pinel, 69675, Bron Cedex, France.

Conflict of Interest: The authors declare no competing financial interest.

Abstract

The desynchronization of alpha and beta oscillations (mu rhythm) in the central scalp EEG during action observation and action execution is thought to reflect neural mirroring processes. However, the extent to which mirror neurons (MNs) or other populations of neurons contribute to such EEG desynchronization is still unknown. Here, we provide the first evidence that, in the monkey, the neuronal activity recorded from the ventral premotor cortex (PMv) strongly contributes to the EEG changes occurring in the beta band over central scalp electrodes, during executed and observed actions. We simultaneously recorded scalp EEG and extracellular activity, Multi Unit Activity (MUA) and Local Field Potentials (LFP), from area F5 of two macaques executing and observing grasping actions. We found that MUA highly correlates with an increase in high gamma LFP power and, interestingly, such LFP power increase also correlates to EEG beta – and in part also to alpha – desynchronization. In terms of timing of signal changes, the increase in high gamma LFP power precedes the EEG desynchronization, during both action observation and execution, thus suggesting a causal role of PMv neuronal activity in the modulation of the alpha and beta mu-rhythm. Lastly, neuronal signals from deeper layers of PMv exert a greater contribution than superficial layers to the EEG beta rhythm modulation, especially during the motor task. Our findings have clear implications for EEG studies in that they demonstrate that the activity of different populations of neurons in PMv contribute to the generation of the mu-rhythm.

Keywords: Action observation, LFP, Mirror neurons, Motor system, Mu rhythm

1 Introduction

The discovery of mirror neurons (MNs) in the monkey cerebral cortex has stimulated the field of cognitive neuroscience by suggesting that these neurons have an active role in encoding others' actions and intentions. The original reports were made through extracellular recording of neurons in the premotor and parietal cortices (Fogassi et al., 2005; Gallese, Fadiga, Fogassi, & Rizzolatti, 1996). The fact that these neurons fire both during the observation of an action and during its execution prompted the idea that they map the visual description of an action onto its cortical motor representation, thus facilitating the process of recognition and imitation of the action performed by others. Reports in humans have described what appears to be neural mirroring using methods that are at best indirect assessments of the presence of MNs. One of these methods, the electroencephalography (EEG), showed that preparation, execution and imagination of movements, or the observation of movements performed by others, desynchronizes EEG oscillations within the alpha (8-13 Hz) and beta (15-30 Hz) frequency bands recorded from electrodes placed over the sensorimotor cortex. These alpha and beta EEG oscillations, also known as the mu rhythm, are thought to reflect neural responses related to the MN system (Cuevas, Cannon, Yoo, & Fox, 2014; Fox et al., 2015a; Muthukumaraswamy, Johnson, & McNair, 2004; Pineda, 2005; Vanderwert, Fox, & Ferrari, 2013a)

Investigations using magnetoencephalography (MEG) have revealed that the mu rhythm results from two different frequency components: one that peaks in the alpha band at around 10 Hz and originates from the primary somatosensory cortex, and another that peaks in the beta band at around 20 Hz and clusters anterior to the central sulcus. This latter component would primarily reflect the contribution of the precentral motor cortex (Riitta Hari & Salmelin, 1997). Several EEG studies in humans confirmed these MEG findings and showed desynchronization in both alpha (Cochin, Barthelemy, Lejeune, Roux,

& Martineau, 1998; Cochin, Barthelemy, Roux, & Martineau, 1999; Muthukumaraswamy & Johnson, 2004) and beta (Avanzini et al., 2012; Babiloni et al., 2002; Muthukumaraswamy & Johnson, 2004) frequencies in central electrodes while subjects executed or observed actions. Thus, both the alpha and beta EEG components may reflect the activation of functional fronto-parietal circuits involved in sensorimotor transformations underlying action production and/or in the processing of visual information related to others' behavior.

Simultaneous EEG and fMRI recordings were used as a first approach aimed at investigating the contribution of MN activity to mu rhythm desynchronization. Using these techniques, Arnstein and colleagues (2011) have found that the activation of different areas, beyond the motor cortex (i.e. primary somatosensory cortex), correlate with the EEG alpha suppression over central electrodes. Also, Ritter and collaborators (2009) have showed an inverse correlation between suppression of the EEG central alpha and fMRI BOLD activity in the postcentral cortex, and also between the EEG beta band suppression and BOLD activity in the precentral cortex. These studies, while suggestive of a relation between mu suppression and MN activity, do not indicate which of the activated areas is the main source that directly causes EEG suppression, and which neuronal population contributes to it. More important, the use of fMRI in those studies made it impossible to know if the neuronal populations involved during action observation and execution included or were related to MNs. No direct evidence of the contribution of MNs to the mu rhythm has ever been explored so far and the link between activity of MNs in premotor and parietal regions and EEG changes recorded at the scalp level is still not understood (Fox et al., 2015a).

In order to fill this gap, here we simultaneously recorded EEG scalp activity and, multiunit activity (MUA) and local field potential (LFP) activity from the PMv cortex of two adult macaque monkeys. The aim of the study was to clarify whether PMv MNs and EEG

desynchronization reflect the same underlying mechanisms during the execution and observation of goal-directed actions. Previous studies have investigated the relation between spiking activity, LFP and EEG signals (Logothetis et al., 2004; Buzsaki et al. 2003). They showed that the action potential from a neuron have a short propagation distance in the extracellular medium and EEG is an emergent signal from activity of a very high number of neurons far more distant. The LFP gamma band instead is an index of spikes' synchrony and can be locked in phase with low frequency oscillations (Logothetis et al., 2004; Buzsaki et al. 2003). This is because there are a large number of neurons that emit spikes in synchrony that generate rhythmic currents in the extracellular medium. Thus, the information carried by the gamma band of LFP is an important connection between the macroscopic activity of EEG and the microscopic activity at the neuronal level (Buzsaki et al, 2012). In our study we therefore first assessed whether the firing activity of mirror neurons and motor neurons in PMv correlated with the LFP activity in the high gamma frequency band. Once this was established, we then analyzed the relation between the high gamma band in the LFP signal and the EEG activity recorded at the scalp level.

2 Materials and Methods

2.1 Animals and surgical procedures

Two captive-born and individually housed adult female rhesus macaques (*Macaca mulatta*) served as subjects. The animal handling, as well as surgical and experimental procedures, complied with the European guidelines (86/609/EEC 2003/65/EC Directives and 2010/63/EU) and Italian laws in force on the care and use of laboratory animals, and were approved by the Veterinarian Animal Care and Use Committee of the University of

Parma (Prot. 78/12 17/07/2012) and authorized by the Italian Health Ministry (D.M. 294/2012-C, 11/12/2012). The monkeys were housed and handled in strict accordance with the recommendations of the Weatherall Report about good animal practice. The well-being and health conditions of the monkeys were constantly monitored by the institutional veterinary doctor of the University of Parma.

A titanium head post (Crist Instrument, Hagerstown, MD, USA) was surgically implanted on the skull using titanium screws. Later, when the monkeys were trained to perform the tasks, a cilux recording chamber (18X18 mm, Alpha-Omega, Israel) was stereotaxically implanted and secured with dental cement. For both procedures, each animal was deeply anaesthetized with ketamine hydrochloride (5 mg/kg i.m.) and medetomidine hydrochloride (0.1 mg/kg i.m.) and his heart rate, temperature and respiration were carefully monitored and kept within physiological range. Pain medication was routinely given after surgery: (Dexamethasone, 2mg/kg, every 12 hours, from 1 day before to 3 days after surgery; Ketoprofen, 5mg/kg, every 12 hours for 3 days following surgery).

2.2 Testing procedures

2.2.1 Grasping execution task (ET)

The task is illustrated in Figure 1A. The monkey sat facing a table (60X60 cm) onto which a metallic cube was placed along the monkey body midline, at 13 cm from monkey's hand starting position. The monkey had to reach and grasp the object and then place it in a small container located 10 cm to the left of the grasping location. At the

beginning of each trial, the monkey had to keep the right hand on a handle attached to the table for at least 1000 ms (Figure1A-I), after which, a transparent barrier was removed to give the “go” signal and the monkey grasped the object (Figure 1A-II) and placed it in the container (Figure 1A-III). A juice reward was delivered after 500-1000 ms, if the monkey correctly executed the trial (Figure 1A-IV). The ET was run in one or more blocks of trials and reached a minimum total of 12 trials per condition. Any trial in which the grasping action was not properly executed was aborted and no reward was delivered.

2.2.2 Grasping observation task (OT)

This task is illustrated in Figure 1B. The monkey SAT facing a table (60X60 cm) onto which two metallic cubes (the target objects) were placed out of the monkey’s reach; one on the right and one on the left side of the experimenter (or corresponding to the ipsi- and contralateral side, with respect to the left side recorded hemisphere). The experimenter (or *agent*) sat at the other end of the table, in front of the monkey, with his right hand resting on a starting pad located on the table between the two targets. The monkey was trained to orient its gaze on the target object, located either on the left or right side of the experimenter (randomly selected and indicated by a laser pointer). A task trial started if the monkey was leaning its hand on the handle (Figure 1B-I). After 1000 ms, the monkey had to fixate the target object (red square) and to maintain fixation for 1000 ms (Figure 1B-II). While the monkey was fixating, the agent grasped the target object (Figure 1B-III). A juice reward was delivered if the monkey correctly fixated the target object for 1000 ms (Figure 1B-IV). The monkey was also required to hold the handle throughout the entire trial to get the reward. The release of the handle automatically aborted the trial and no reward was delivered. Within the OT, we implemented a further condition- *No grasp*

condition (NG)- in order to control for possible attentional factors. In this condition the agent seated in front of the monkey but did not perform any grasping and kept his hand on the starting platform throughout the trial. The monkey was required to fixate the target object and to hold the handle throughout the entire trial to get the reward, as in the OT task.

2.3 Task control

Contact-detecting electric circuits (Crist Instruments, MD, USA) and a PC equipped with a customized LabView® software (National Instruments, USA) were employed in order to monitor and control every aspects of the tasks and align all neuronal signals with behavioral events. The recorded events were: a) contact of the monkey/experimenter's hand with the starting point; b) detachment of the monkey/experimenter's hand from the starting point; c) contact of the monkey/experimenter's hand with the grasping target. The monkey's eye position was monitored by means of a customized eye-tracking system composed by a 50 Hz CCD camera (Ganz, model ZC-F11CH4) and two spots of infrared light. The eye position signal was processed through a dedicated software (University of Tübingen, Germany) and fed to the Lab-View® software to be monitored and recorded.

2.4 Data recording

All neural signals were recorded with a 16-channel Omniplex Neural Data Acquisition System (Plexon inc, TX, USA) with a sampling frequency of 40 KHz. Eight channels were dedicated to MUA and LFP recordings using a linear multielectrode array (LMA; U-probe, Plexon inc., TX, USA) with eight microelectrodes (15μm diameter and 250μm spacing)

embedded in a stainless needle. Each electrode's impedance ranged from 0.5 to 1.5 MΩ (measured at 1 KHz). The most superficial electrode was maintained at the subdural level during recordings and served as reference electrode, while the remaining seven electrodes were dedicated to multiunit and LFP recordings. Eight additional channels were used for EEG recordings and were connected to an external bioamplifier (James Long Company, NY, USA). The EEG signal was amplified, band-pass filtered from 0.1 to 100 Hz, sampled at 1 KHz, and recorded through the Omniplex recording system. The EEG signal was recorded with a customized lycra cap (Electro-Cap International, OH, USA) designed to fit around the recording chamber for neuronal activity and leave it accessible for MUA and LFP recordings. The EEG cap was fitted with seven tin electrodes, with impedances kept under 20 kΩ and measured at 1 KHz. The electrodes were referenced to an eighth electrode, localized at the vertex, and grounded to the U-Probe stainless needle to limit noise and artifacts.

2.5 Preliminary testing of neuronal activity

Before proceeding with the neuronal testing using our testing procedures, single and multiunit activity were systematically tested for visuomotor properties to identify recording sites endowed with MNs activity (Maranesi et al., 2012a; Rozzi, Ferrari, Bonini, Rizzolatti, & Fogassi, 2008). Briefly, we required the monkey to grasp food items in various conditions (i.e. with eyes closed, or without flexing the wrist, elbow or shoulder) enabling us to disentangle neuronal activity related to visual stimulation, reaching or grasping objects. Also, to exclude the possible presence of mouth-related responses, we tested any neural activity changes related to the delivery of small pieces of food directly into the mouth while the monkeys' eyes were closed. Finally, visual properties were studied by presenting the monkeys with 3D-objects (e.g. food items and solids) of different shapes,

sizes and orientations, moved in various space locations, direction and distances from the monkey, as well as different manual actions performed by the experimenter.

2.6 Data pre-processing

MUA was extracted from raw neuronal recordings with the application of a forward-reverse Butterworth high pass filter at 1 KHz, followed by a spike detection procedure selecting only action potentials with an amplitude between 3 and 15 standard deviations (SD) of the estimated signal noise. Histograms describing the spiking activity were calculated with a bin width of 10 ms and smoothed with a linear Gaussian filter (σ = 5 bins). The same raw data were used to detect LFP with a forward-reverse Butterworth low pass filter at 500 Hz, followed by a down-sampling of data from 40 KHz to 1KHz (to match EEG data). Finally a linear whitening filter (Staude, 2001) and a 50 Hz notch filter were applied in order to filter out pink noise common component of the signals. The raw EEG signal was down-sampled to 250 Hz in order to remove power spectral density (PSD) distortion above 100 Hz, due to the bio-amplifier internal filter. A linear whitening filter was applied, and the signal was up-sampled to 1 KHz to match the LFP sampling frequency. Finally, a 50 Hz notch filter was applied.

2.7 Behavioral epochs

All recorded brain signals were analyzed and compared considering two epochs – *baseline* and *stimulus* – of 500 ms duration for each task. The *baseline* epoch for both ET and OT was recorded during the first 500 ms of the trial, when the monkey remained still and was leaning her hand on the handle. The *stimulus* epoch for ET started at the

monkey's hand approaching and contacting the object and ended 500 ms later, while for OT it corresponded to the 500 ms preceding the agent's hand contact with the target object.

2.8 Spectral analysis

All data pre-processing and analyses were performed in Matlab (R2013A, Mathworks, USA). Multi-taper spectrograms, for both LFP and EEG, were calculated, using *Chronux* – a Matlab-based software package (Mitra & Bokil, 2008) – on data segments of 7 sec, centered on the agent (OT) or the monkey (ET) hand's contact with the object. Signals were band-pass filtered from 7 Hz to 100 Hz. All spectrograms were computed using a moving window of 1 sec (time step=10 ms) with a bandwidth of 3 Hz and using 5 tapers. The baseline PSD was subtracted to every calculated time – frequency bin of the spectrograms expressed in dB. All trials were averaged. Three frequency bands were considered for all subsequent data analyses: EGG alpha (7-15 Hz), EEG beta (15-31 Hz) and LFP high gamma (63-100 Hz).

2.9 Correlation analysis

The correlation analysis between spiking activity and EEG was performed in two steps. In the first step, we aligned spike emission and LFP power using the Spike Triggered Time Frequency Average (STTFA) method (Ray, Hsiao, Crone, Franaszczuk, & Niebur, 2008). The STTFA was calculated by first creating LFP segments of 7 seconds around the emission of each spike. All spike-centered LFP segments were then averaged for each trial and across all trials. To compensate for the time–frequency components that are not phase-locked to the spikes, the STTFA data needed to be normalized. This normalization

consisted in subtracting a randomized STTFA (rSTTFA) from the original STTFA data (dSTTFA). The rSTTFA was created by calculating an STTFA on randomly generated spikes.

The normalized STTFA – here denoted nSTTFA – was calculated as follows:

$$nSTTFA = 10\ (\log_{10}(dSTTFA) - \log_{10}(rSTTFA))$$

This analysis was performed on the data recorded from all microelectrode depths.

In a second step of our correlation analysis, we calculated Pearson's correlation coefficients between LFP and EEG power. The Pearson correlation coefficients were calculated between LFP (high gamma) and EEG (alpha and beta) signals as follows:

$$corr(Y_{EEG}, Y_{LFP}) = \frac{\sigma_{Y_{EEG}Y_{LFP}}}{\sigma_{Y_{EEG}}\sigma_{Y_{LFP}}}$$

where:

$$Y_{EEG} = 10\ (\log_{10}(S_{EEG}) - \log_{10}(B_{EEG})),$$
$$Y_{LFP} = 10\ (\log_{10}(S_{LFP}) - \log_{10}(B_{LFP}))$$

and B, S denote PSD for *stimulus* and *baseline*, respectively. The correlation maps were obtained using the Pearson correlation coefficients and interpolating the EEG electrode positions with cubic splines. We used a significance criterion of $p<0.05$ in all maps. Once the maps were constructed, the significance level of the Pearson's correlation across the entire maps was calculated with linear interpolation of the correlation coefficients with the probability close to the significance criterion ($p<0.05$). This criterion was then used to establish the color threshold for significant data. Note that the color threshold is different between ET (yellow) and OT (green) due to difference in trial number.

2.10 Time-course analysis of alpha and beta EEG activity and high gamma LFP activity.

We performed a time course analysis in order to detect the onset time of the rise of high-gamma LFP activity and the onset time of the alpha and beta EEG suppression, for ET, OT and *No-grasp*. Note that the *No-grasp* condition was subtracted from OT, in order to remove any signal changes not directly related to the observed grasping actions. We then used the onset time values to calculate the latency time between LFP increase and EEG suppression for both ET and OT-*No Grasp*.

The EEG and LFP time-frequency data from each electrode were first averaged across all trials and then multiple Wilcoxon rank – sum tests were applied, along the entire trial duration, between the baseline activity (50 bins of 10 ms), from 1250 ms to 750 ms before the hand's contact with the object, and a 100 ms moving window (10 bins of 10 ms), with a time step of 10 ms. The Bonferroni correction for multiple comparisons was applied to all Wilcoxon rank – sum tests.

The onset time of both EEG suppression and LFP increase was defined as the first time after 10 consecutive statistically significant tests. Finally, the onset times were averaged across the four central EEG electrodes and across all the seven LFP electrode depths and the difference between the resulting values was calculated to detect the LFP-EEG latency time.

2.11 Statistical analysis

The mean PSD for stimulus and baseline epochs were calculated in each trial for the EEG and the LFP. The statistical significance of the difference between stimulus and baseline was calculated using paired-sample *t*-tests separately for each frequency band of interest

(alpha, beta, low-gamma and high gamma). A significance criterion of p<0.05 was used.

The nSTTFA standard error (SE_{nSTTFA}) were calculated for every trial, using the following formula:

$$SE_{nSTTFA} = \frac{10}{\log_e 10} \sqrt{\frac{\left(\frac{\sigma_{dSTTFA}}{dSTTFA}\right)^2 + \left(\frac{\sigma_{rSTTFA}}{rSTTFA}\right)^2}{n\_spikes}}$$

Where σ_{dSTTFA} and σ_{rSTTFA} are, respectively, the standard deviation of direct and randomized STTFA over all spikes in every trial, and n_spikes is the number of spikes in every trial.

2.12 Histological assessment of recording sites

At the end of the neurophysiological experiments, electrolytic lesions (10 lA cathodic pulses per 10 s) were performed in one monkey at known coordinates, in order to delimit the external borders of the studied region and to allow the subsequent anatomical reconstruction of the penetration grid. At 1 week after the lesions, the monkey was anaesthetized with ketamine hydrochloride (15 mg／kg, i.m.) followed by intravenous lethal injection of pentobarbital sodium and perfused through the left cardiac ventricle with saline, 3.5–4% paraformaldehyde and 5% glycerol in this order, prepared in phosphate buffer 0.1 M, pH 7.4. The brain was then removed from the skull, photographed, cryoprotected, and then frozen and cut in coronal sections. Each second and fifth section of a series of five was stained using the Nissl method (Maranesi et al., 2012b).

Subsequently, the cytoarchitectonic features of the primary motor and premotor cortices were identified according to the criteria of Belmalih and colleagues (2007, 2009). In particular, the convexity of area F5, in its most rostral part, is characterized by a relatively

poor lamination, by an overall small cell size of layer III and V pyramids, and by a radial organization in layers II, V and VI. Considering that cytoarchitectonic features often change gradually from one region to another, the borders between adjacent areas have been established based on previous published work (Maranesi et al., 2012b).

3 Results

Neuronal spiking activity and LFP signals were recorded from the hand sector of area F5 of the left hemisphere of two behaving macaques. We first characterized the neuronal properties of F5 area through systematic testing. After having identified the cortical sector containing MNs, we carried out a series of cortical penetrations in which single unit, MUA and LFP were simultaneously recorded with scalp EEG. This report includes data from four recording sessions (i.e. four multielectrode penetrations, each paired with EEG scalp recording). Overall, we analyzed the data from a total of 104 trials for the grasping execution task (ET) (50 trials in M1 and 54 in M2) and 151 trials for the grasping observation task (OT) (65 trials in M1 and 86 in M2).

Figure 2 illustrates the results of the EEG, LFP and MUA recordings. First, we found a robust task-related EEG power spectrum density (PSD) modulation. Specifically, the EEG spectrograms showed a statistically significant decrease in power in the alpha and beta frequency bands (blue color, $p<0.05$), for anterior and central electrodes (number 1 to 5, Figure 2B) during both ET and OT. In contrast, an increase in power (red and yellow color, $p<0.05$) was found in beta, gamma and high gamma frequency bands over the posterior scalp locations (number 6 and 7, Figure 2B). The mean MUA firing rate is presented in Figure 2C (black lines overlaying the spectrograms). Overall, for all microelectrodes, the firing rate increases and reaches a peak when the hand of the

monkey (ET) or the experimenter (OT) touches the target object (dashed vertical lines). The firing rate during the grasping epochs (see *Behavioral epochs* in *Methods section*), averaged across all electrodes (not showed), was significantly different from their respective *baselines* in ET (baseline=38.9 ± 1.7 Hz, stimulus=71.5 ± 2.5 Hz, t=7.95, df = 12, p <0.0001) and in OT (baseline=43.1 ± 1.2 Hz, stimulus=61.9 ± 0.6 Hz, t=9.60, df = 12, p <0.0001; paired two-tailed t-test), confirming that we recorded neurons with clear motor and mirror properties. Finally, LFP spectrograms (Figure 2C, color maps) showed a significant increase of the PSD in the high gamma frequency band and a significant decrease in the beta frequency band, around the hand contact with the object (vertical dashed lines), for both tasks (ET and OT) and in all microelectrodes.

3.1 Correlations between MUA and LFP

To analyze the relationship between MUA spiking activity and the LFP differential power (see *Spectral analysis* in the *Materials and Methods* section), we calculated the normalized Spike Triggered Time Frequency Average (nSTTFA), which consists in the averaged power spectrum of the LFP associated with spike emission (see *Correlation analysis* in *Methods section*). We included an average of 21162 and 33755 spikes for each microelectrode in ET and OT, respectively. Figure 3 shows the result of the nSTTFA where the red to yellow color maps denote significant LFP power increase (p<0.01) associated with spike emission and implies a positive correlation, while the blue color range represents significant power decrease (p<0.01) implying a negative correlation. The green color represents values that did not show any significant change in power (in dB). We observed a high and positive correlation between LFP in the high gamma band and spiking activity at all microelectrodes depths. Spikes and LFP high gamma oscillatory

signals showed an increase in activity during both ET and OT, thus validating the use of LFP high gamma activity as a reliable index of MNs MUA spiking activity.

3.2 Correlations between LFP and EEG

We implemented a series of Pearson's correlations in order to correlate LFP's high gamma activity with EEG activity in the alpha and beta bands at each scalp location (Figure 4; See also the same plot for the two separated monkeys on Supplementary Figure 1 and 2). The colors represent the correlation coefficients and the significance thresholds (ST) of the correlations for $p<0.05$ (ST = -0.19 (yellow) for ET; ST = -0.16 (green) for OT). The correlation maps between the EEG alpha and LFP high gamma bands did yield few significant values over central-frontal electrodes, which are somehow more evident in the correlation matrix of non-interpolated data (See Supplementary Figure 3). However, extensive and significant negative correlations were found between EEG beta and LFP high gamma frequency bands, during both ET and OT tasks (See also correlation matrix in Supplementary Figure 3). Indeed, for ET we found an inverse correlation between the central EEG electrodes and the microelectrodes located at 750 to 1250 μm in the cortex, while for OT the inverse correlation involved central and frontal EEG electrodes and microelectrodes spreading from 250 to 1500 μm in depth.

3.3 LFP and EEG time course analysis

We compared the onset time of high gamma LFP power increase to that of the alpha and beta EEG power decrease (Figure 5; see also two examples of time course in Supplementary Figure 4). If the EEG desynchronization was appearing simultaneously or

in anticipation to the onset of LFP increase, we would conclude that neuronal activity in the PMv cortex has little or no contribution to the generation of the EEG desynchronization recorded over the central electrodes. We found instead that during the ET the mean onset of the LFP power increase preceded EEG desynchronization in the alpha band by 840 ms (+/- 10) and in the beta band by 143 ms (+/- 22). We observed an anticipation of LFP increase compared to the onset of EEG desynchronization also in OT. For the alpha band the latency was 544 ms (+/- 102) while for beta band it was 145 ms (+/- 68).

3.4 Histological assessment

In order to approximately assess at which cortical depth the different microelectrodes were recording from, we performed a histological analysis of the convexity of F5 in one monkey. Through photographic analysis, we overlaid the linear multieloectrode array layout on the Nissl-stained section of the recorded region. This allowed us to identify from which cortical layers the different microelectrodes were recording and therefore to clarify whether the correlations between LFP and EEG signals were associated with neuronal activity generated from superficial or deeper cortical layers. This analysis revealed that, on average, the array with its 8 microelectrodes could record at different depths covering all the 6 cortical layers (Figure 6). Although there is variability in the cortical organization of the layers in the F5 convexity, it was possible to estimate the positions of some electrodes in relation to the histological properties of the PMv cortex. The results showed that our recording sites ranged in depth from 250μm to 1750μm. In particular, we found that electrodes placed between 1000μm to 1500 μm were more likely recording from the 5th cortical layer which is characterized by relatively high density of pyramidal cells.

4 Discussion

This study is the first to investigate the relationship between spiking activity of PMv neurons and simultaneously scalp recorded EEG mu rhythm. It shows that the activity of mirror and motor neurons recorded from the PMv contributes to the EEG mu rhythm desynchronization occurring over central scalp locations, during action execution and observation.

4.1 Specificity of EEG desynchronization during action execution and observation

The EEG data revealed a significant desynchronization in power recorded from central electrodes in the alpha and beta frequency bands for both ET and OT tasks, and, in contrast, a strong synchronization in these frequency bands over posterior electrodes. These results are consistent with - and extend to action execution - previous findings from our lab showing desynchronization in the beta band during grasping observation in adult monkeys (Coudé et al., 2014). They are also in line with human EEG and MEG studies in literature describing desynchronization in both the alpha and beta bands during action observation (Hari et al. 1997, 1998; Cochin et al. 1998; Babiloni et al. 2002; Muthukumaraswamy and Johnson 2004a, 2004b; Muthukumaraswamy et al. 2004). Importantly, the EEG bands, here described as sensitive to action execution and action observation, are similar in both their spectral and topographical characteristics to the alpha (around 10 Hz) and beta (around 20 Hz) bands that have been extensively described in the investigations of the human mirror system (Rizzolatti, Cattaneo, Fabbri-Destro, & Rozzi, 2014; Vanderwert, Fox, & Ferrari, 2013b).

Although scalp EEG activity recorded in particular electrodes does not necessarily reflect the cortical activity that is taking place directly below them, the prominence of mu desynchronization for action execution and in central sites that overlay the sensorimotor cortex has led researchers to consider mu desynchronization as an index of motor and/or somatosensory cortical activation. Indeed, a recent meta-analysis of over 70 such studies (Fox et al., 2015b) found evidence for topographical specificity to central electrode locations for mu ERD only for execution but not for observation. The current data indicate that, at least in the non-human primate, there is a topographic specificity of EEG frequencies during action execution and observation and that this event-related desynchronization is correlated with neuronal activity in the PMv.

4.2 Local field potentials as a marker of spiking activity

We found that on average the spike emission was positively correlated with the increase in LFP power within the high gamma band, across different cortical depths. The link between spiking activity and LFP has been supported by several investigations showing that the power increase in LFP high frequencies (>40 Hz) may reflect the firing rate of small neuronal populations lying near each recording electrode (Goense & Logothetis, 2008; Katzner et al., 2009; Ray, Crone, Niebur, Franaszczuk, & Hsiao, 2008; Ray, Hsiao, et al., 2008; Ray & Maunsell, 2011; Whittingstall & Logothetis, 2009; Xing, Yeh, & Shapley, 2009) together with other non-synaptic events (Kocsis, Bragin, & Buzsáki, 1999).

The increase of the high gamma LFP power in PMv, during action observation, probably reflects the increase of the spiking activity recorded at multiunit and single cell level, and may be the result of the activity of MN populations in the hand sector of F5, similarly to what was also found by Caggiano and colleagues (Caggiano, Giese, Thier, &

Casile, 2015). However, a stronger correlation between high gamma LFP and spiking activity during action execution could be the result of the activation of more than one neuronal population. In fact, it is possible that in addition to MNs, purely motor neurons, which represent the great majority of the neurons in this sector (Maranesi et al., 2012a), contribute to the multiunit activity and LFP signals recorded during action execution.

4.3 Action execution/observation, LFP and EEG desynchronization

Partly in line with our expectations, the data show that there are weak significant correlations between LFP high gamma increase and EEG alpha desynchronization in both ET and OT. These results were somehow expected, but the correlations were relatively modest, considering the broad literature describing desynchronization in the alpha band as a marker of mirror activity (Fox et al., 2015b; Muthukumaraswamy et al., 2004). Our data therefore support this view only in part. However, the current findings should be viewed within a particular frame. First, we only recorded extracellular activity in the PMv while MNs are located within a broader cortical network (Bonini, 2015) which includes the parietal cortex. It is therefore possible that mirror activity in the parietal cortex better correlates with scalp recorded EEG changes in the alpha band. In fact, other studies using EEG, ECoG, MEG or combining fMRI and EEG have found that alpha desynchronization is correlated with parietal activity or likely generated in the parietal cortex, with the somatosensory cortex as a possible main cortical source (Andrew & Pfurtscheller, 1997; Arnstein et al., 2011; Babiloni et al., 1999; Crone et al., 1998; Hari, 2006; Pfurtscheller, 2003; Pfurtscheller & Berghold, 1989; Pfurtscheller, Neuper, Andrew, & Edlinger, 1997; Pfurtscheller, Zalaudek, & Neuper, 1998). Clearly, further studies should attempt to

reconcile the different results generated with different methodological approaches in order to understand the nature of these cortical oscillations.

An important finding of this study is the strong inverse correlation between high gamma LFP activity and beta EEG desynchronization during both execution and observation of grasping actions. During execution, the correlations were specifically distributed over the central electrodes and the highest correlation coefficient was present at 1250μm. Histological assessments confirmed that the highest levels of correlation between LFP and EEG were present in electrodes mainly located around deeper cortical layers (likely around the 5^{th}), which are characterized by rich pyramidal cells and represents the main motor output of this cortical sector. It is therefore likely that EEG desynchronization within the beta band during ET is the result of the activity of populations of motor neurons in the PMv cortex associated with the control of grasping movements. However, our data do not exclude the possibility that other cortical sectors contribute to the source of this signal. Our data also confirm findings first presented by Hari and colleagues (1997; 1998) in which they reported, using MEG with human participants, beta desynchronization in the PMv cortex during both action execution and action observation. More recent studies showed that observing and executing actions recruit a broader network which includes, in addition to the classical parietal-premotor network, the intraparietal sulcus, the primary motor cortex, the dorsal premotor cortex, and the supplementary motor areas (Bonini, 2015; Bruni et al. 2017). Thus, neurons in the PMv might represent one key hub of this extended mirror network contributing, more or less directly, to the EEG mu rhythm desynchronization.

For OT, the correlations were more distributed across different microelectrode depths than for ET, likely including the 2^{nd} and 3^{rd} layers. The highest level of LFP-EEG correlation was present over the central EEG electrodes, while it was not significant over

the occipital electrodes. The fact that the correlations are extended across different microelectrodes depths possibly reflects the activity of a broader cortical network, with input and output currents from/to the PMv cortex that contribute to the generation of the EEG desynchronization recorded over central electrodes during action observation. The analysis of the time course of LFP and EEG activity showed that during grasping execution and observation the LFP power increase in the high gamma band anticipates the EEG desynchronization in both the alpha and beta bands. This finding would be compatible with the idea that the neuronal activity in the premotor cortex could play an important role in the generation of the signal recorded at the level of the scalp in the central electrodes. However, it must be noted that the timing of anticipation of LFP in the beta band is shorter (approximately 150 ms for both the OT and ET) than the alpha band (approximately 550 ms for the OT and 850 ms for the ET). Such finding could be interpreted by the fact that the spiking activity of neurons in F5 probably have a more profound impact on the brain structures that are nearby the recording electrodes, and could contribute to the rapid EEG changes observed in the beta band. Longer latencies observed between LFP-alpha EEG compared to LFP-beta EEG probably reflect the fact that the brain activity changes recorded over the scalp are linked to a network that is less functionally connected to the premotor cortex. This result would further support the correlation analysis discussed previously, and overall would further strengthen the hypothesis that the EEG desynchronization within the beta frequency band has its main source in the motor cortex. Further studies, however, should better investigate the possible causal link between LFP activity and the EEG desynchronization.

These findings represent the first evidence that the activation of neurons in the PMv cortex correlates with EEG desynchronization in the beta band. This supports the hypothesis that the pattern of desynchronization within this specific EEG frequency band is an important marker of neuronal activity and, more specifically, that it is highly correlated

with the activity of MNs in the PMv cortex during action observation. There is growing evidence from MEG and ECoG studies that the beta rhythm originates predominantly in the motor cortex (Collinger et al., 2014; Crone et al., 1998; Hari et al., 1997; Hari, 2006). Most of these studies have investigated this rhythm during the planning or the performance of voluntary movements and through the analysis of cortex-muscle coherence in isometric muscle contraction (Salenius, Portin, Kajola, Salmelin, & Hari, 1997). Studies using MEG have consistently found desynchronization around 20 Hz over the primary motor cortex during observation, hearing and execution of actions involving the hand or the mouth (Caetano, Jousmäki, & Hari, 2007; Hari et al., 1998; Järveläinen, Schürmann, & Hari, 2004; Nishitani & Hari, 2002). Our data for ET support these findings. The OT data seems to only partly support this hypothesis as the correlation pattern seems to be more distributed along the different depths of the cortex, thus suggesting that during action observation, the PMv could represent an important node in a network that likely involves other cortical areas. Therefore, not only the neuronal output, but also the input from other regions seems to be important in contributing to the EEG beta desynchronization.

The pattern of correlation between high gamma LFP and EEG found during grasping observation revealed two important features: 1) it is more distributed at different electrode depths, and 2) it is more prominent in the anterior/central electrodes. Since we have recorded in an area previously selected for the richness of MNs at all electrode depths, it is very likely that the type of neurons that contribute to this pattern are MNs. However, the presence of such correlation at all cortical depths suggests that both the input and the output from area F5 might contribute to generate the EEG desynchronization.

Acknowledgements: This research was supported by NICHD grant (NIH P01HD064653).

References

Andrew, C., & Pfurtscheller, G. (1997). On the existence of different alpha band rhythms in the hand area of man. *Neuroscience Letters*, *222*(2), 103–6. Retrieved from http://www.ncbi.nlm.nih.gov/pubmed/9111739

Arnstein, D., Cui, F., Keysers, C., Maurits, N. M., & Gazzola, V. (2011). -Suppression during Action Observation and Execution Correlates with BOLD in Dorsal Premotor, Inferior Parietal, and SI Cortices. *Journal of Neuroscience*, *31*(40), 14243–14249. http://doi.org/10.1523/JNEUROSCI.0963-11.2011

Avanzini, P., Fabbri-Destro, M., Dalla Volta, R., Daprati, E., Rizzolatti, G., & Cantalupo, G. (2012). The dynamics of sensorimotor cortical oscillations during the observation of hand movements: An EEG study. *PLoS ONE*, *7*(5), e37534. http://doi.org/10.1371/journal.pone.0037534

Babiloni, C., Babiloni, F., Carducci, F., Cincotti, F., Cocozza, G., Del Percio, C., … Rossini, P. M. (2002). Human cortical electroencephalography (EEG) rhythms during the observation of simple aimless movements: A high-resolution EEG study. *NeuroImage*, *17*(2), 559–572. http://doi.org/10.1016/S1053-8119(02)91192-4

Babiloni, C., Carducci, F., Cincotti, F., Rossini, P. M., Neuper, C., Pfurtscheller, G., & Babiloni, F. (1999). Human movement-related potentials vs desynchronization of EEG alpha rhythm: a high-resolution EEG study. *NeuroImage*, *10*(6), 658–65. http://doi.org/10.1006/nimg.1999.0504

Belmalih, A., Borra, E., Contini, M., Gerbella, M., Rozzi, S., & Luppino, G. (2007). A multiarchitectonic approach for the definition of functionally distinct areas and domains in the monkey frontal lobe. *Journal of Anatomy*, *211*(2), 199–211.

http://doi.org/10.1111/j.1469-7580.2007.00775.x

Belmalih, A., Borra, E., Contini, M., Gerbella, M., Rozzi, S., & Luppino, G. (2009). Multimodal architectonic subdivision of the rostral part (area F5) of the macaque ventral premotor cortex. *The Journal of Comparative Neurology*, *512*(2), 183–217. http://doi.org/10.1002/cne.21892

Bonini, L. (2015). The extended mirror neuron network: Anatomy, origin, and functions. *Neuroscientist*. http://doi.org/10.1002/elan.

Caetano, G., Jousmäki, V., & Hari, R. (2007). Actor's and observer's primary motor cortices stabilize similarly after seen or heard motor actions. *Proceedings of the National Academy of Sciences of the United States of America*, *104*(21), 9058–62. http://doi.org/10.1073/pnas.0702453104

Caggiano, V., Giese, M., Thier, P., & Casile, A. (2015). Encoding of point of view during action observation in the local field potentials of macaque area F5. *European Journal of Neuroscience*, *41*(4), 466–476. http://doi.org/10.1111/ejn.12793

Cochin, S., Barthelemy, C., Lejeune, B., Roux, S., & Martineau, J. (1998). Perception of motion and qEEG activity in human adults. *Electroencephalography and Clinical Neurophysiology*, *107*(4), 287–295. http://doi.org/10.1016/S0013-4694(98)00071-6

Cochin, S., Barthelemy, C., Roux, S., & Martineau, J. (1999). Observation and execution of movement: Similarities demonstrated by quantified electroencephalography. *European Journal of Neuroscience*, *11*(5), 1839–1842. http://doi.org/10.1046/j.1460-9568.1999.00598.x

Collinger, J. L., Vinjamuri, R., Degenhart, A. D., Weber, D. J., Sudre, G. P., Boninger, M. L., … Wang, W. (2014). Motor-related brain activity during action observation: a neural substrate for electrocorticographic brain-computer interfaces after spinal cord

injury. *Frontiers in Integrative Neuroscience*, *8*, 17. http://doi.org/10.3389/fnint.2014.00017

Coudé, G., Vanderwert, R. E., Thorpe, S., Festante, F., Bimbi, M., Fox, N. a, … B, P. T. R. S. (2014). Frequency and topography in monkey electroencephalogram during action observation : possible neural correlates of the mirror neuron system. *Philosophical Transactions of the Royal Society B*, *369*, 20130415. http://doi.org/10.1098/rstb.2013.0415

Crone, N. E., Miglioretti, D. L., Gordon, B., Sieracki, J. M., Wilson, M. T., Uematsu, S., & Lesser, R. P. (1998). Functional mapping of human sensorimotor cortex with electrocorticographic spectral analysis. I. Alpha and beta event-related desynchronization. *Brain : A Journal of Neurology*, *121 (Pt 1*, 2271–2299. http://doi.org/10.1093/brain/121.12.2271

Cuevas, K., Cannon, E. N., Yoo, K., & Fox, N. A. (2014). The infant EEG mu rhythm: Methodological considerations and best practices. *Developmental Review*, *34*(1), 26–43. http://doi.org/10.1016/j.dr.2013.12.001

Fogassi, L., Ferrari, P. F., Gesierich, B., Rozzi, S., Chersi, F., & Rizzolatti, G. (2005). Parietal lobe: from action organization to intention understanding. *Science (New York, N.Y.)*, *308*(5722), 662–667. http://doi.org/10.1126/science.1106138

Fox, N. A., Bakermans-Kranenburg, M. J., Yoo, K. H., Bowman, L. C., Cannon, E. N., Vanderwert, R. E., … van IJzendoorn, M. H. (2015a). Assessing Human Mirror Activity With EEG Mu Rhythm: A Meta-Analysis. *Psychological Bulletin*. http://doi.org/10.1037/bul0000031

Fox, N. A., Bakermans-Kranenburg, M. J., Yoo, K. H., Bowman, L. C., Cannon, E. N., Vanderwert, R. E., … van IJzendoorn, M. H. (2015b). Assessing Human Mirror Activity With EEG Mu Rhythm: A Meta-Analysis. *Psychological Bulletin*.

http://doi.org/10.1037/bul0000031

Gallese, V., Fadiga, L., Fogassi, L., & Rizzolatti, G. (1996). Action recognition in the premotor cortex. *Brain : A Journal of Neurology*, *119 (Pt 2*, 593–609. http://doi.org/10.1093/brain/119.2.593

Goense, J. B. M., & Logothetis, N. K. (2008). Neurophysiology of the BOLD fMRI Signal in Awake Monkeys. *Current Biology*, *18*(9), 631–640. http://doi.org/10.1016/j.cub.2008.03.054

Hari, R. (2006). Action-perception connection and the cortical mu rhythm. *Progress in Brain Research*, *159*(6), 253–60. http://doi.org/10.1016/S0079-6123(06)59017-X

Hari, R., Forss, N., Avikainen, S., Kirveskari, E., Salenius, S., & Rizzolatti, G. (1998). Activation of human primary motor cortex during action observation: a neuromagnetic study. *Proceedings of the National Academy of Sciences of the United States of America*, *95*(25), 15061–15065. http://doi.org/10.1073/pnas.95.25.15061

Hari, R., & Salmelin, R. (1997). Human cortical oscillations: A neuromagnetic view through the skull. *Trends in Neurosciences*, *20*(1), 44–49. http://doi.org/10.1016/S0166-2236(96)10065-5

Hari, R., Salmelin, R., Mäkelä, J. P., Salenius, S., & Helle, M. (1997). Magnetoencephalographic cortical rhythms. *International Journal of Psychophysiology*, *26*(1–3), 51–62. http://doi.org/10.1016/S0167-8760(97)00755-1

Järveläinen, J., Schürmann, M., & Hari, R. (2004). Activation of the human primary motor cortex during observation of tool use. *NeuroImage*, *23*(1), 187–92. http://doi.org/10.1016/j.neuroimage.2004.06.010

Katzner, S., Nauhaus, I., Benucci, A., Bonin, V., Ringach, D. L., & Carandini, M. (2009). Local Origin of Field Potentials in Visual Cortex. *Neuron*, *61*(1), 35–41.

http://doi.org/10.1016/j.neuron.2008.11.016

Kocsis, B., Bragin, a, & Buzsáki, G. (1999). Interdependence of multiple theta generators in the hippocampus: a partial coherence analysis. *The Journal of Neuroscience : The Official Journal of the Society for Neuroscience*, *19*(14), 6200–6212.

Maranesi, M., Rodà, F., Bonini, L., Rozzi, S., Ferrari, P. F., Fogassi, L., & Coudé, G. (2012a). Anatomo-functional organization of the ventral primary motor and premotor cortex in the macaque monkey. *European Journal of Neuroscience*, *36*(10), 3376–3387. http://doi.org/10.1111/j.1460-9568.2012.08252.x

Maranesi, M., Rodà, F., Bonini, L., Rozzi, S., Ferrari, P. F., Fogassi, L., & Coudé, G. (2012b). Anatomo-functional organization of the ventral primary motor and premotor cortex in the macaque monkey. *European Journal of Neuroscience*, *36*(10), 3376–3387. http://doi.org/10.1111/j.1460-9568.2012.08252.x

Mitra, P., & Bokil, H. (2008). Observed Brain Dynamics. *Convergence*, *43*(2), xxii, 381 . http://doi.org/10.1093/acprof:oso/9780195178081.001.0001

Muthukumaraswamy, S. D., & Johnson, B. W. (2004). Changes in rolandic mu rhythm during observation of a precision grip. *Psychophysiology*, *41*(1), 152–156. http://doi.org/10.1046/j.1469-8986.2003.00129.x

Muthukumaraswamy, S. D., & Johnson, B. W. (2004). Primary motor cortex activation during action observation revealed by wavelet analysis of the EEG. *Clinical Neurophysiology : Official Journal of the International Federation of Clinical Neurophysiology*, *115*(8), 1760–6. http://doi.org/10.1016/j.clinph.2004.03.004

Muthukumaraswamy, S. D., Johnson, B. W., & McNair, N. a. (2004). Mu rhythm modulation during observation of an object-directed grasp. *Cognitive Brain Research*, *19*(2), 195–201. http://doi.org/10.1016/j.cogbrainres.2003.12.001

Nishitani, N., & Hari, R. (2002). Viewing lip forms: cortical dynamics. *Neuron*, *36*(6), 1211–20. Retrieved from http://www.ncbi.nlm.nih.gov/pubmed/12495633

Pfurtscheller, G. (2003). Induced oscillations in the alpha band: functional meaning. *Epilepsia*, *44 Suppl 1*, 2–8. http://doi.org/12001 [pii]

Pfurtscheller, G., & Berghold, a. (1989). Patterns of cortical activation during planning of voluntary movement. *Electroencephalography and Clinical Neurophysiology*, *72*(3), 250–258. http://doi.org/10.1016/0013-4694(89)90250-2

Pfurtscheller, G., Neuper, C., Andrew, C., & Edlinger, G. (1997). Foot and hand area mu rhythms. In *International Journal of Psychophysiology* (Vol. 26, pp. 121–135). http://doi.org/10.1016/S0167-8760(97)00760-5

Pfurtscheller, G., Zalaudek, K., & Neuper, C. (1998). Event-related beta synchronization after wrist, finger and thumb movement. *Electroencephalography and Clinical Neurophysiology*, *109*(2), 154–60. Retrieved from http://www.ncbi.nlm.nih.gov/pubmed/9741806

Pineda, J. a. (2005). The functional significance of mu rhythms: Translating “seeing” and “hearing” into “doing.” *Brain Research Reviews*, *50*(1), 57–68. http://doi.org/10.1016/j.brainresrev.2005.04.005

Ray, S., Crone, N. E., Niebur, E., Franaszczuk, P. J., & Hsiao, S. S. (2008). Neural correlates of high-gamma oscillations (60-200 Hz) in macaque local field potentials and their potential implications in electrocorticography. *The Journal of Neuroscience : The Official Journal of the Society for Neuroscience*, *28*(45), 11526–11536. http://doi.org/10.1523/JNEUROSCI.2848-08.2008

Ray, S., Hsiao, S. S., Crone, N. E., Franaszczuk, P. J., & Niebur, E. (2008). Effect of stimulus intensity on the spike-local field potential relationship in the secondary

somatosensory cortex. *The Journal of Neuroscience : The Official Journal of the Society for Neuroscience*, *28*(29), 7334–7343. http://doi.org/10.1523/JNEUROSCI.1588-08.2008

Ray, S., & Maunsell, J. H. R. (2011). Different origins of gamma rhythm and high-gamma activity in macaque visual cortex. *PLoS Biology*, *9*(4). http://doi.org/10.1371/journal.pbio.1000610

Ritter, P., Moosmann, M., & Villringer, A. (2009). Rolandic alpha and beta EEG rhythms' strengths are inversely related to fMRI-BOLD signal in primary somatosensory and motor cortex. *Human Brain Mapping*, *30*(4), 1168–1187. http://doi.org/10.1002/hbm.20585

Rizzolatti, G., Cattaneo, L., Fabbri-Destro, M., & Rozzi, S. (2014). Cortical mechanisms underlying the organization of goal-directed actions and mirror neuron-based action understanding. *Physiological Reviews*, *94*(2), 655–706. http://doi.org/10.1152/physrev.00009.2013

Rozzi, S., Ferrari, P. F., Bonini, L., Rizzolatti, G., & Fogassi, L. (2008). Functional organization of inferior parietal lobule convexity in the macaque monkey: electrophysiological characterization of motor, sensory and mirror responses and their correlation with cytoarchitectonic areas. *The European Journal of Neuroscience*, *28*(8), 1569–88. http://doi.org/10.1111/j.1460-9568.2008.06395.x

Salenius, S., Portin, K., Kajola, M., Salmelin, R., & Hari, R. (1997). Cortical control of human motoneuron firing during isometric contraction. *Journal of Neurophysiology*, *77*(6), 3401–5. Retrieved from http://www.ncbi.nlm.nih.gov/pubmed/9212286

Staude, G. H. (2001). Precise onset detection of human motor responses using a whitening filter and the log-likelihood-ratio test. *IEEE Transactions on Biomedical Engineering*, *48*(11), 1292–1305. http://doi.org/10.1109/10.959325

Vanderwert, R. E., Fox, N. a., & Ferrari, P. F. (2013a). The mirror mechanism and mu rhythm in social development. *Neuroscience Letters*, *540*, 15–20. http://doi.org/10.1016/j.neulet.2012.10.006

Vanderwert, R. E., Fox, N. A., & Ferrari, P. F. (2013b). The mirror mechanism and mu rhythm in social development. *Neuroscience Letters*, *540*, 15–20. http://doi.org/10.1016/j.neulet.2012.10.006

Whittingstall, K., & Logothetis, N. K. (2009). Frequency-Band Coupling in Surface EEG Reflects Spiking Activity in Monkey Visual Cortex. *Neuron*, *64*(2), 281–289. http://doi.org/10.1016/j.neuron.2009.08.016

Xing, D., Yeh, C.-I., & Shapley, R. M. (2009). Spatial spread of the local field potential and its laminar variation in visual cortex. *The Journal of Neuroscience : The Official Journal of the Society for Neuroscience*, *29*(37), 11540–11549. http://doi.org/10.1523/JNEUROSCI.2573-09.2009

Legends

Figure 1 Tasks. A) Grasping execution task (ET). A-I) The monkey has his right hand at rest on the starting handle for at least 1000ms (baseline). A transparent barrier is in place between the monkey and the target object. A-II) The barrier is removed (go signal). The monkey is reaching and grasping the target object; A-III) The monkey places the object in the container; A-IV) A liquid reward is delivered if the task is successfully executed. B) Grasping observation task (OT). B-I) The agent and the monkey have their hands in the starting position; B-II) The monkey fixates the target object; B-III) The agent grasps the object; B-IV) The monkey receives a liquid reward if the trial is correctly executed.

Figure 2 Simultaneous recording of EEG from scalp electrodes, and of MUA and LFP from a linear multielectrode array (LMA) during grasping execution (ET) and observation (OT).

A) Schematic view of the monkey head with approximate position of scalp electrodes and single-unit recording chamber. In inset, diagram of LMA layout indicating relative electrode depth. B) Spectrograms of the EEG signal recorded from seven different sites on the scalp. Yellow and red colors denote significant power increase (synchronization), while blue color shows significant power decrease (desynchronization). Green color denotes not significant variations. In inset: enlarged view of two EEG spectrograms. C) Spectrograms of LFPs (color map) and MUA histograms (black line) recorded at different electrodes. In inset: enlarged view of two LFP spectrograms/MUA histograms. For all graphs the activity is aligned with the hand contact with the target object during grasping (indicated by the vertical dashed line at time = 0). The horizontal dashed lines separate the frequency bands of interest (from top to bottom: high gamma – not showed for EEG, low gamma, beta and alpha).

Figure 3. Spike-Triggered Time-Frequency Average (STTFA). The color maps represent the averaged PSD of the LFPs time-aligned with neuronal spike emission (time = 0). Yellow and red colors represent significant PSD increase (i.e. direct correlation PSD-spike emission), while blue color denotes significant PSD decrease (i.e. inverse correlation PSD-spike emission). *p* values <0.01.

Figure 4. Maps of Pearson's correlation coefficients calculated between the LFP high gamma band, recorded at each microelectrode, and the EEG alpha and beta bands desynchronization, recorded at each EEG scalp location. The significance thresholds are in the yellow color range for ET and in the green color range for OT. *p* values <0.05.

Figure 5. Mean latency (in milliseconds +/- SEM) between the onset time of EEG desynchronization and LFP power increase.

Figure 6. Histological assessment. (A) Lateral view drawing of the macaque brain; the dashed line indicates the level at which the coronal section, shown in B, was taken. (B)

Coronal section drawing where the dashed box indicates the location of the photomicrograph shown in C. (C) Photomicrograph of the Nissl-stained section. (D) Schematic drawing of the linear multielectrode array (LMA) superimposed on a high magnification view of the cytoarchitectonic area F5c. The location of the photomicrograph is indicated by the dashed box in the photomicrograph shown in C. Roman numerals correspond to the different cortical layers. White squares indicate the relative depth (in μm) of the LMA electrodes. C, central sulcus; Cg, cingulate sulcus; IA, inferior arcuate sulcus; IP, intraparietal sulcus; L, lateral sulcus; Lu, lunate sulcus; P, principal sulcus; SA, superior arcuate sulcus; ST, superior temporal sulcus.

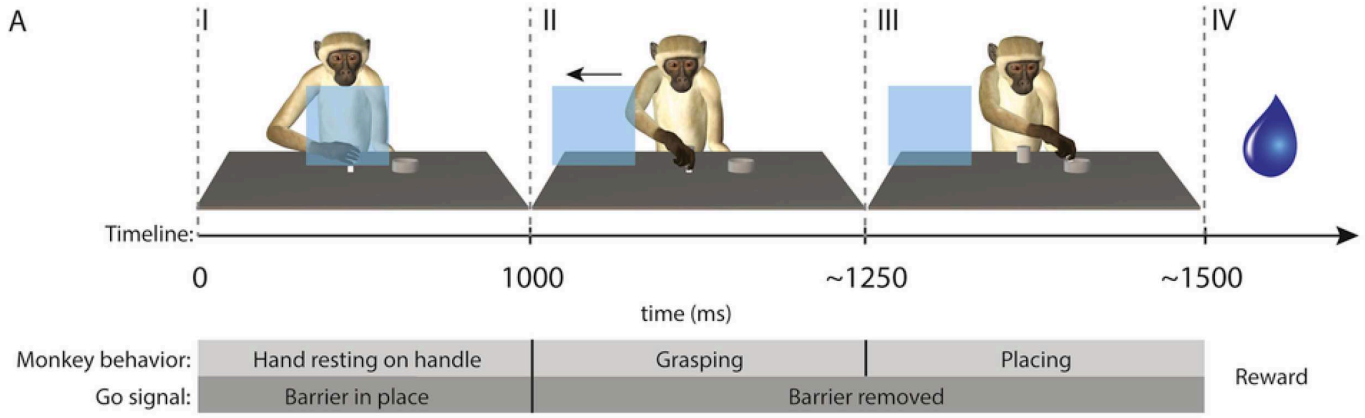
A
I
II
III
IV
Timeline:
0
1000
~1250
~1500
time (ms)
Monkey behavior:
Hand resting on handle
Grasping
Placing
Go signal:
Barrier in place
Barrier removed
Reward

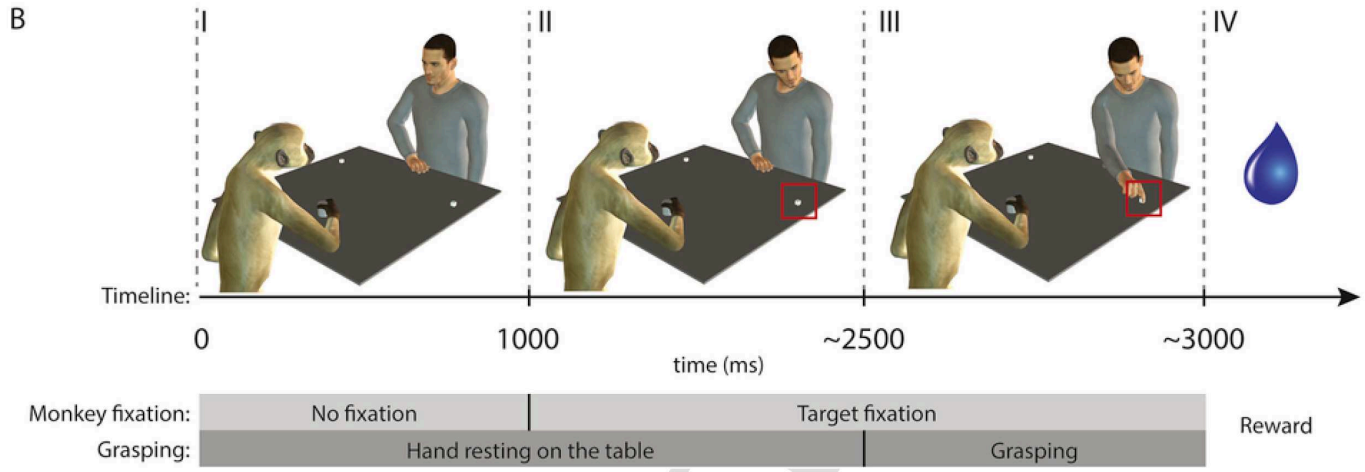
B
I
II
III
IV
Timeline:
0
1000
~2500
~3000
time (ms)
Monkey fixation:
No fixation
Target fixation
Grasping:
Hand resting on the table
Grasping
Reward

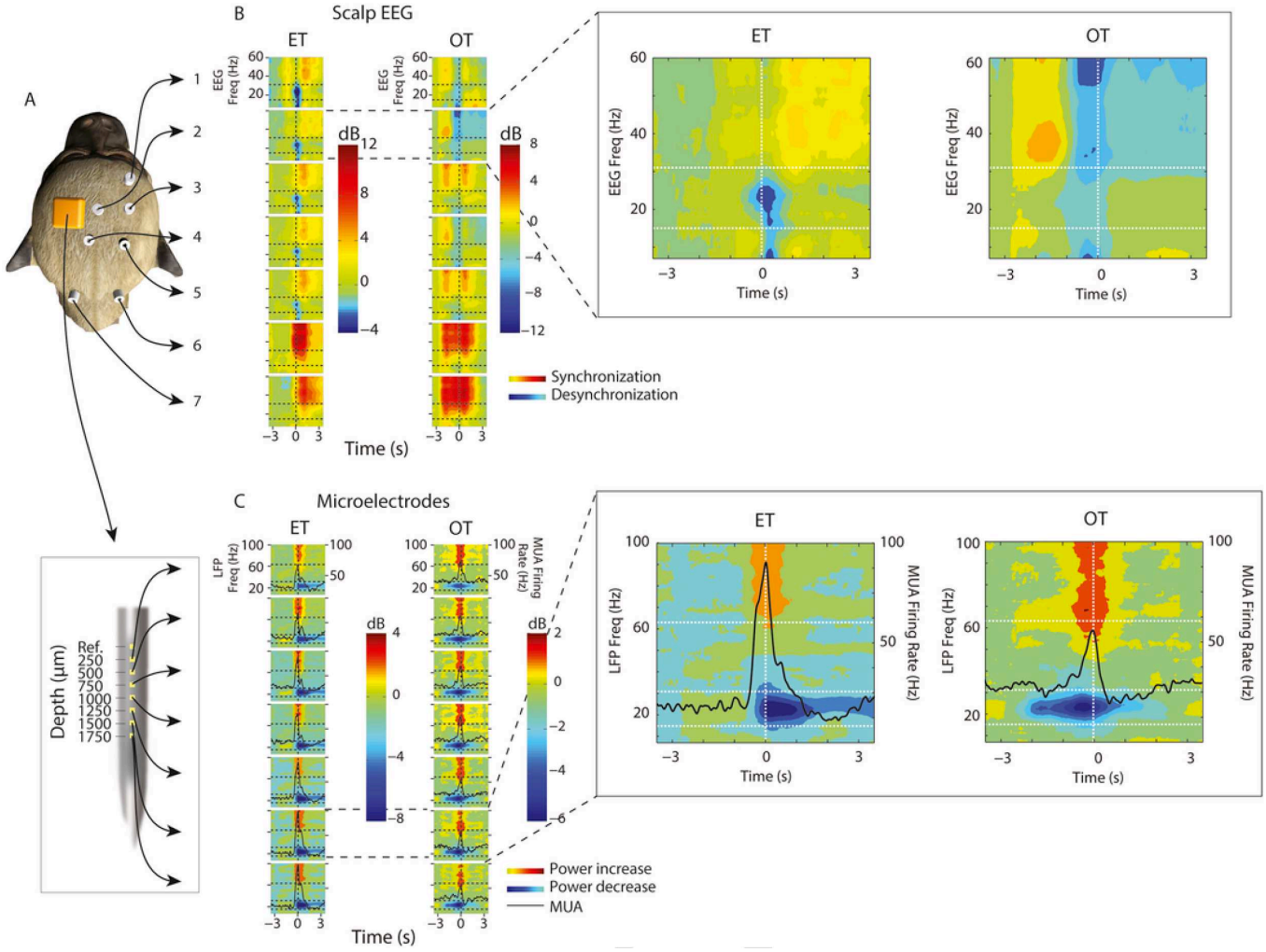
A
1
2
3
4
5
6
7
B
Scalp EEG
ET
OT
EEG Freq (Hz)
60
40
20
dB
12
8
4
0
−4
−8
−12
Time (s)
−3
0
3
Synchronization
Desynchronization
C
Microelectrodes
LFP Freq (Hz)
MUA Firing Rate (Hz)
100
60
20
50
Depth (μm)
Ref.
250
500
750
1000
1250
1500
1750
Power increase
Power decrease
MUA

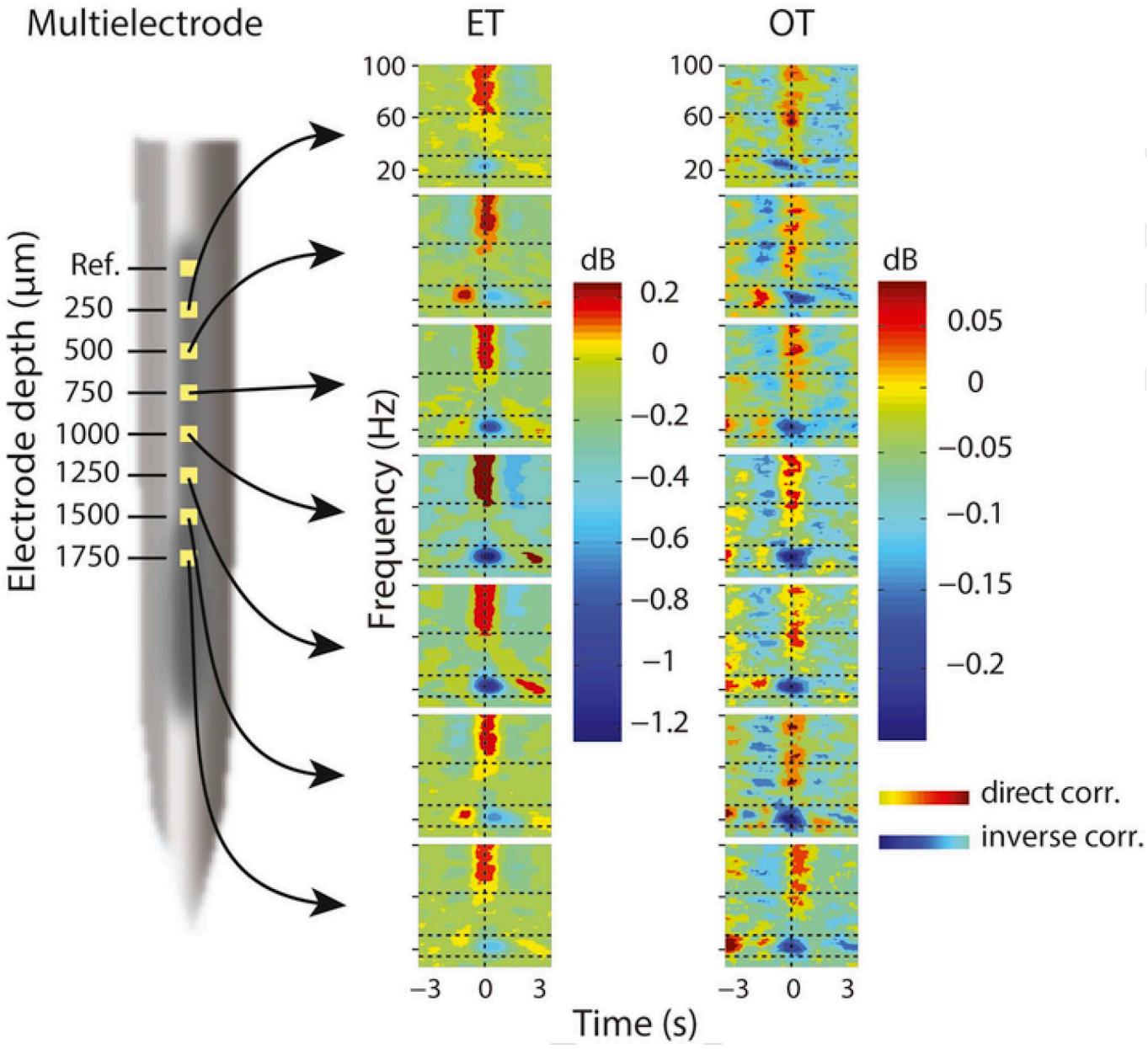
Multielectrode
ET
OT
Electrode depth (µm)
Ref.
250
500
750
1000
1250
1500
1750
Frequency (Hz)
100
60
20
dB
0.2
0
−0.2
−0.4
−0.6
−0.8
−1
−1.2
0.05
−0.05
−0.1
−0.15
−0.2
direct corr.
inverse corr.
−3
0
3
Time (s)

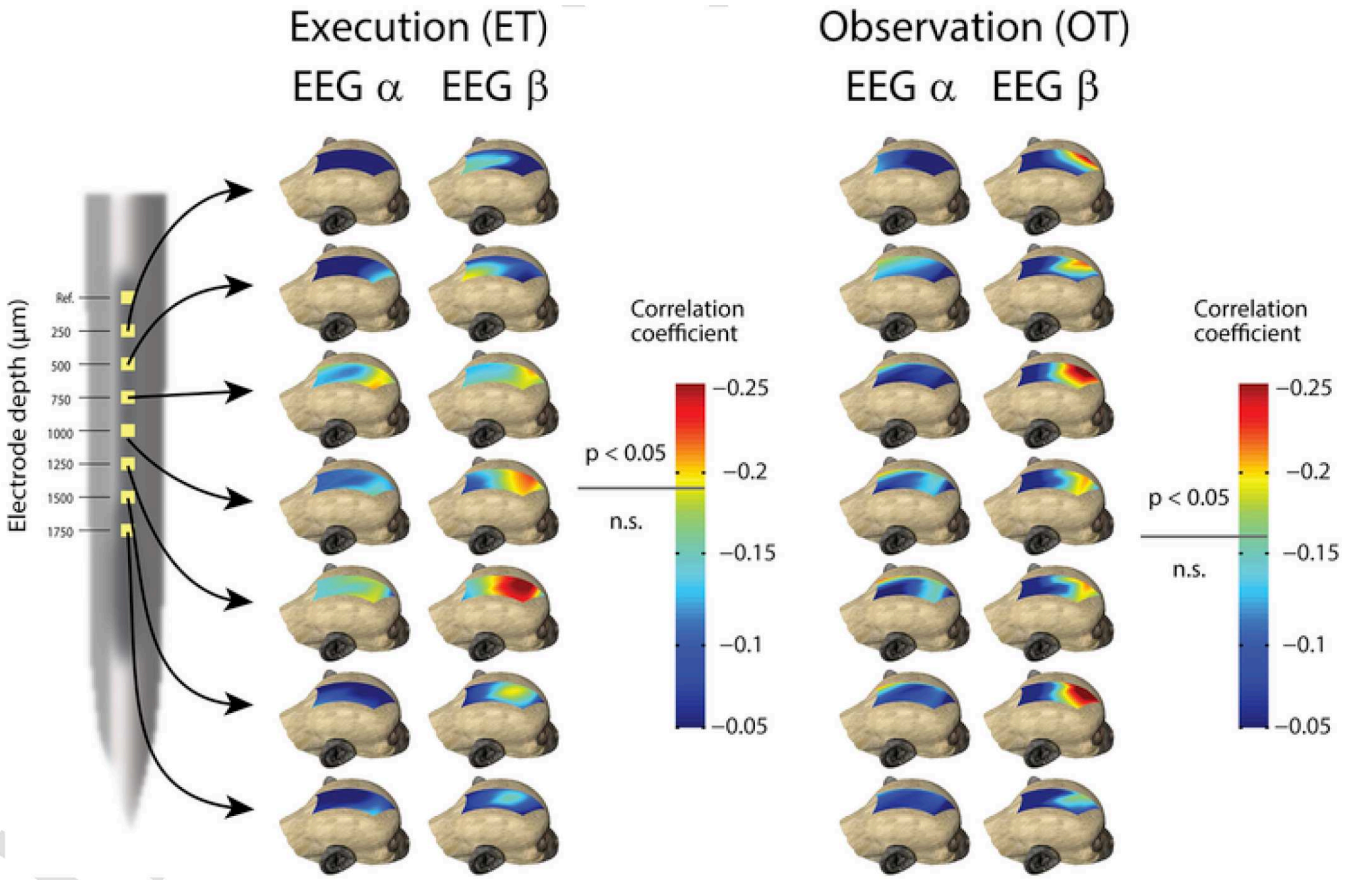
Execution (ET)
EEG α
EEG β
Observation (OT)
EEG α
EEG β
Electrode depth (μm)
Ref.
250
500
750
1000
1250
1500
1750
Correlation coefficient
−0.25
−0.2
−0.15
−0.1
−0.05
p < 0.05
n.s.
Correlation coefficient
−0.25
−0.2
−0.15
−0.1
−0.05
p < 0.05
n.s.

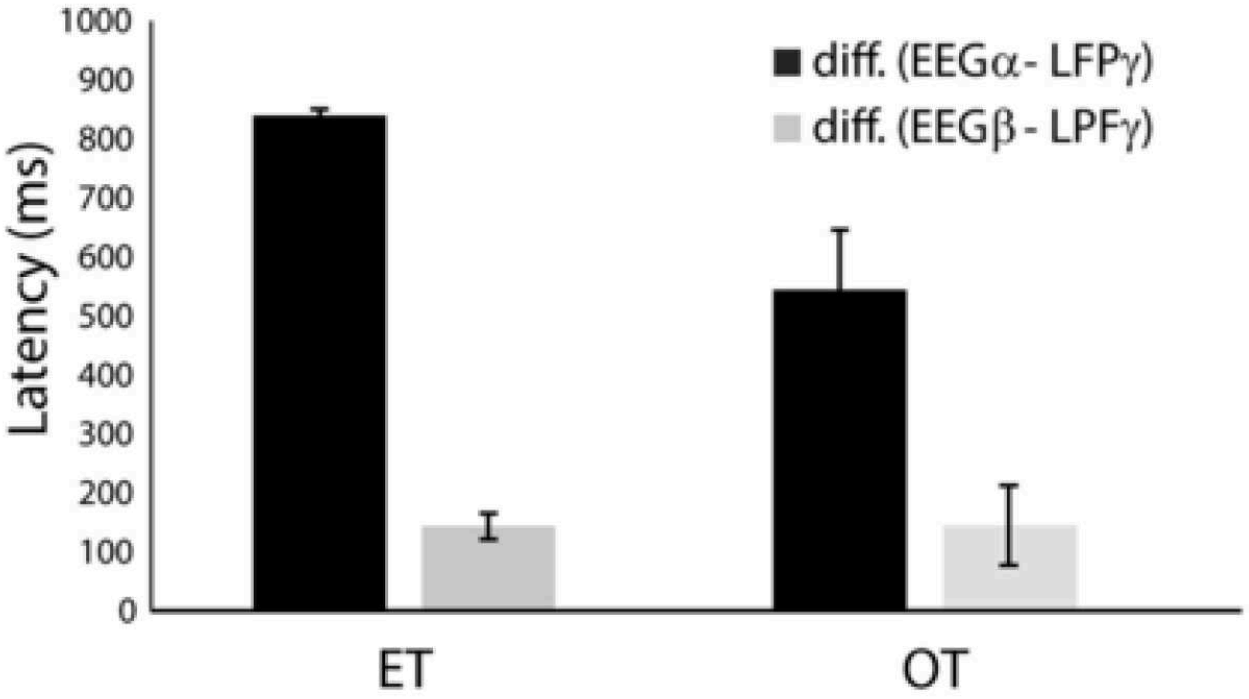
1000
900
800
700
600
500
400
300
200
100
0
Latency (ms)
diff. (EEGα- LFPγ)
diff. (EEGβ - LPFγ)
ET
OT

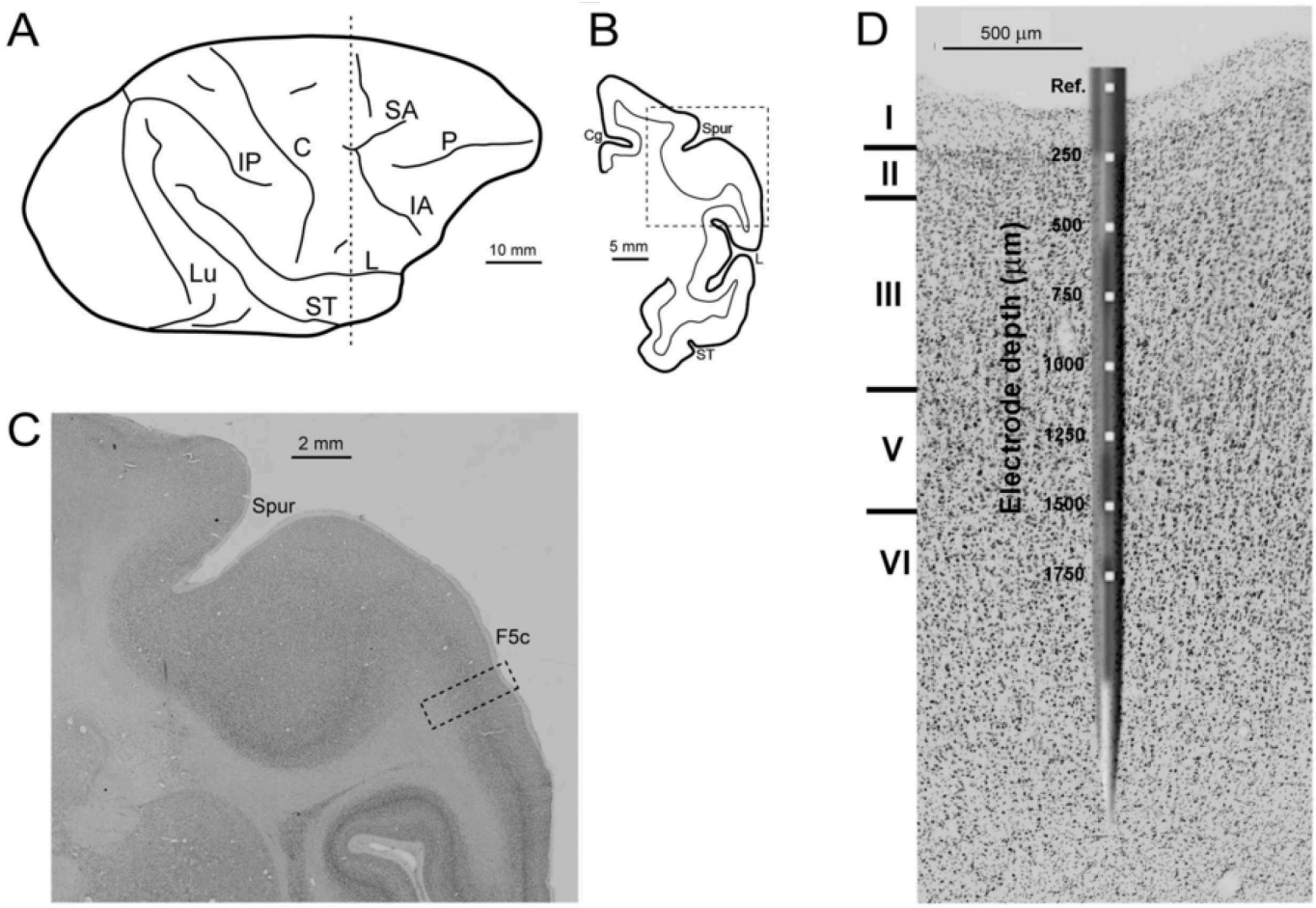
A
SA
P
C
IP
IA
L
Lu
ST
10 mm
B
Cg
Spur
5 mm
L
ST
C
2 mm
Spur
F5c
D
500 µm
Ref.
I
II
III
V
VI
250
500
750
1000
1250
1500
1750
Electrode depth (µm)